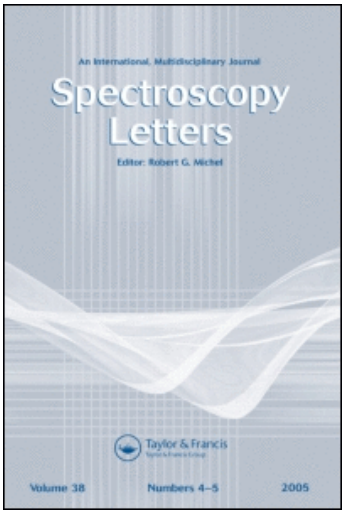

Spectroscopy Letters
Publication details, including instructions for authors and subscription information:
http://www.informaworld.com/smpp/title~content=t713597299

Infrared and Raman Study of the Local Anesthetic Procaine

M. Alcolea Palafox[a]
[a] Departamento de Quimica-Fisica I (Espectroscopia). Facultad de Ciencias Quimicas, Universidad Complutense de Madrid, Madrid, SPAIN

To cite this Article Palafox, M. Alcolea(1994) 'Infrared and Raman Study of the Local Anesthetic Procaine', Spectroscopy Letters, 27: 5, 613 — 638
To link to this Article: DOI: 10.1080/00387019408000857
URL: http://dx.doi.org/10.1080/00387019408000857

SPECTROSCOPY LETTERS, 27(5), 613-638 (1994)

INFRARED AND RAMAN STUDY OF THE LOCAL ANESTHETIC PROCAINE

KEY WORDS: Infrared spectrometry, Raman spectrometry, Anesthetics, Procaine, AM1

M. Alcolea Palafox

Departamento de Quimica-Física I (Espectroscopia). Facultad de Ciencias Químicas. Universidad Complutense de Madrid. Madrid 28040. SPAIN.

ABSTRACT

The infrared and Laser Raman spectra of procaine with free basis in the solid state were obtained. The characteristic vibrational frequencies of their different modes were identified and assigned from isotope shifts and theoretical calculations. An infrared study in the liquid phase was also carried out. The corresponding rotation and inversion barriers in *p*-amino group were computed by means of different optimization procedures.

INTRODUCTION

Several theories[1] exist in the literature on the mode of action[2] in local anaesthetics, the phenomena of drug resistance and toxicity. Information on the interaction[3] of local anaesthetics with phospholipids and lipoprotein

parts of the membrane can be obtained at the molecular level by spectroscopic investigations[4] on structural changes of the system. As a first step in these investigations, the Infrared (IR) and Raman spectra of several local anesthetics have been reported[5]. Procaine (2-diethyl-aminoethyl ester 4-amino benzoic acid) is another local anesthetic that has important pharmaceutical applications.

X-ray studies of procaine[6] (PRC) and its different derivatives[7] show a structure remarkably similar to natural compounds actively participating in nerve impulse transmission. The conformation of the alkylamino end of the molecule, the quinonoidal character of the *p*-aminobenzoate group, and the proximity of the carbonyl oxygen to the ammonium nitrogen are considered to be necessary for an effective interaction with the receptor[8].

In the present paper, the vibrational spectra and the molecular and conformational aspects of PRC, especially in the *p*-amino group, were studied, in order to throw more light on the relationship between structure and activity in local anesthetics.

EXPERIMENTAL

Samples of procaine were obtained from Merck at the highest purity available (99%) and used without further purification. D_2O was obtained from Junta de Energia Nuclear (Spain) with a purity of 99.7%. Deuteration of the samples was carried out using several methods[5,9].

Infrared absorption spectra of samples in KBr pellets were recorded using a Perkin-Elmer 599B spectrophotometer, which is connected to a computer. For the study of the solid-liquid change, the samples were warmed with a thermocouple in a cell with external windows of KBr, using the automatic temperature controller CTC-250 (Beckman). The scale employed ranged from room temperature to 200°C.

The Raman spectra were recorded with spectral slit widths of 100-400 μm on a Ramanor Model U-1000 Raman spectrophotometer using a Spectra Physics 165 Ar^+ ion Laser, at 100-400 mW power.

COMPUTATIONAL METHODS

All AM1[10] calculations were performed with the VAX/IV2 version of AMPAC 2.1 program package[11,12]. The CNDO/2 semiempirical method with standard parametrization[13] was also considered to optimize the geometry of the amino groups and several selected torsional angles.

To evaluate graphically the correctness of starting geometries prior to computation and to review the resulting optimized structure after calculation, the DRAW program was used[14], carried out in a Tektronic 4105 model, a high-resolution graphics computer terminal.

RESULTS AND DISCUSSION

GEOMETRY OPTIMIZATION

The geometry of the PRC molecule in its optimum conformation and the geometric parameters obtained with the AM1 method are shown in Fig. 1. The intermolecular hydrogen bonds formed in the crystal structure of PRC are presented in Fig. 2. The geometry of the molecule, especially of the *p*-amino group, was theoretically optimized, and a *tilt* angle ε of 3.6° of the C-N bond with respect to the plane of the aromatic ring was identified.

VIBRATIONAL SPECTRA

SOLID STATE

The infrared spectra of non-deuterated and deuterated solid PRC are illustrated in Figs. 3-4, while the Raman spectra are given in Figs. 5-7. The frequencies of the bands, their intensities estimated and the assignments are listed in Table 1.

(N-H) stretching vibrations: Since C_{2v} symmetry is assigned to the *p*-amino group, most of the vibrations observed by IR spectroscopy were detected in Raman. In IR, the symmetric and antisymmetric N-H stretching modes

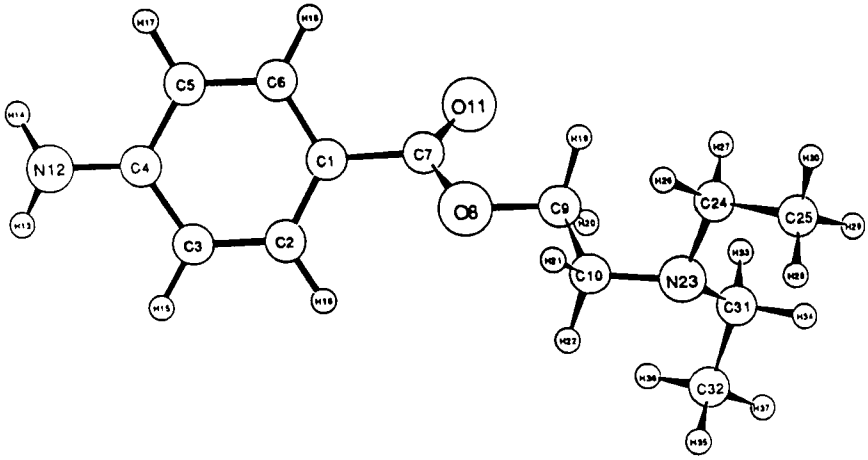

Fig. 1. Optimum geometry of PRC computed by AM1.

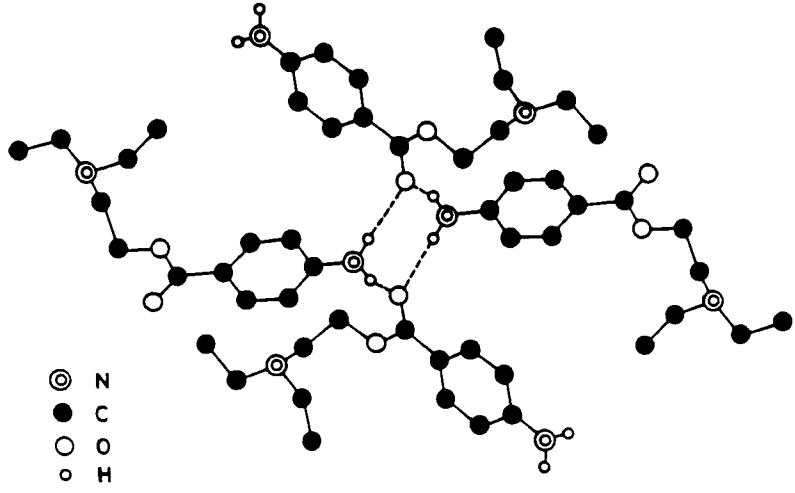

Fig. 2. Intermolecular hydrogens bonds in the crystal structure of PRC.

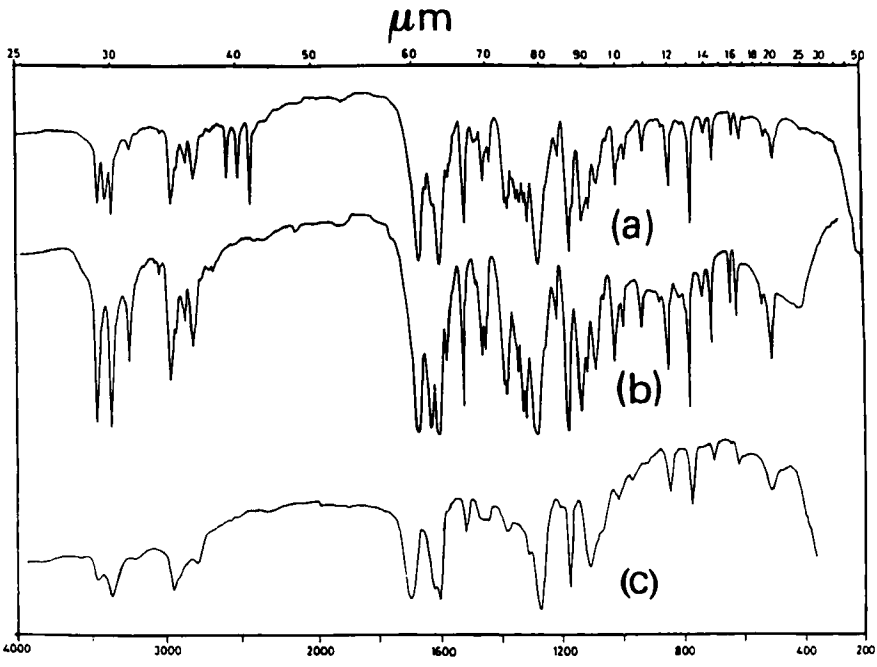

Fig. 3. Infrared spectrum of the PRC a) in the solid state, deuterated, b) in the solid state, non-deuterated, and c) in the liquid phase at 75°C near melting point.

were assigned to the bands at 3360 and 3458 cm^{-1} (3371.5 and 3453.5 cm^{-1} in Raman) respectively, the intensity of the $\nu_s(NH_2)$ mode being higher than the $\nu_{as}(NH_2)$. These frequencies (as in Raman) are not in accordance with the Krueger-Thompson relationship[15], $\nu_s^{cal.} - \nu_s^{exp.} = 21\ cm^{-1}$. This discrepancy is compatible with the existence of intermolecular hydrogen bonds. Thus, the band at 3240 cm^{-1} in IR could be interpreted as vibrations in N-H groups

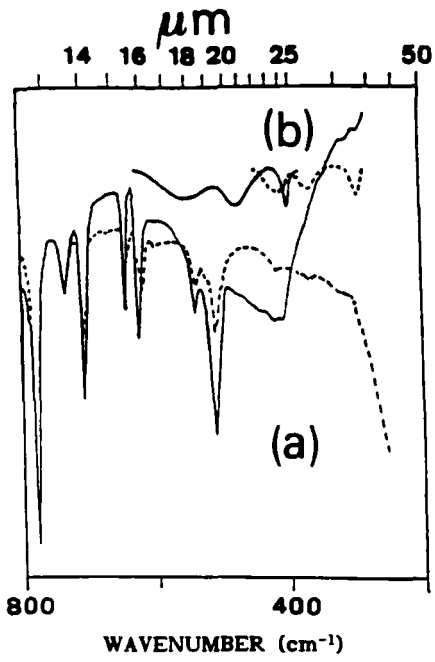

Fig. 4. A detail of the IR spectrum in the 200-800 cm^{-1} range of the solid state of PRC. a) deuterated (broken line) and non-deuterated (solid line), b) substracting the nondeuterated and deuterated spectra in a computer program.

associated with intermolecular hydrogen bonds, or as Fermi resonance between the overtone of the $\delta(NH_2)$ mode and $\nu_s(NH_2)$.

The apparent decrease in intensity on deuteration of the antisymmetric and symmetric stretching bands of the free NH_2 is smaller than the band at 3240 cm^{-1} (IR), which was reasonably attributed to the relative stabilities of the N-H···O intermolecular hydrogen bonds in the crystal. Thus the hydrogens that belong to the intermolecular bonds are more easily exchanged by deuterium than are those pertaining to the free amino groups.

Fig. 3b, shows new bands, sharp and relatively intense, at 2590 and 2438 cm^{-1} corresponding to $\nu_{as}(N\text{-}D)$ and $\nu_s(N\text{-}D)$ in ND_2 groups, respectively. The NH/ND relation is 1.333 and 1.380 in the antisymmetric and symmetric modes respectively, as in the Raman spectrum. The frequency splitting in ND_2 is greater than in NH_2, with a ratio NH_2/ND_2: 0.64, far from that reported[16] in aniline 0.73.

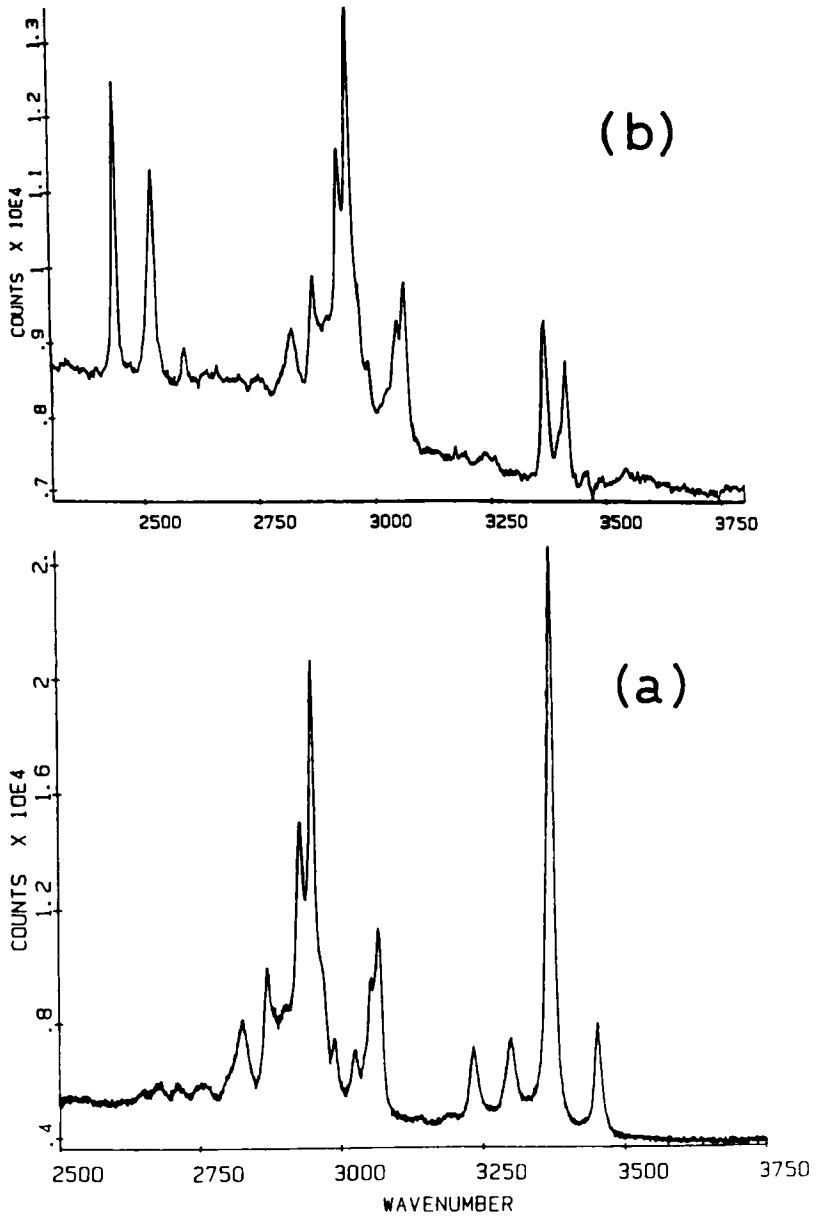

Fig. 5. Raman spectra a) of the non-deuterated PRC in solid state with laser power of 300 mw and slits = 400 μm. b) of the deuterated PRC in the solid state with laser power = 400 mw and slits = 400 μm.

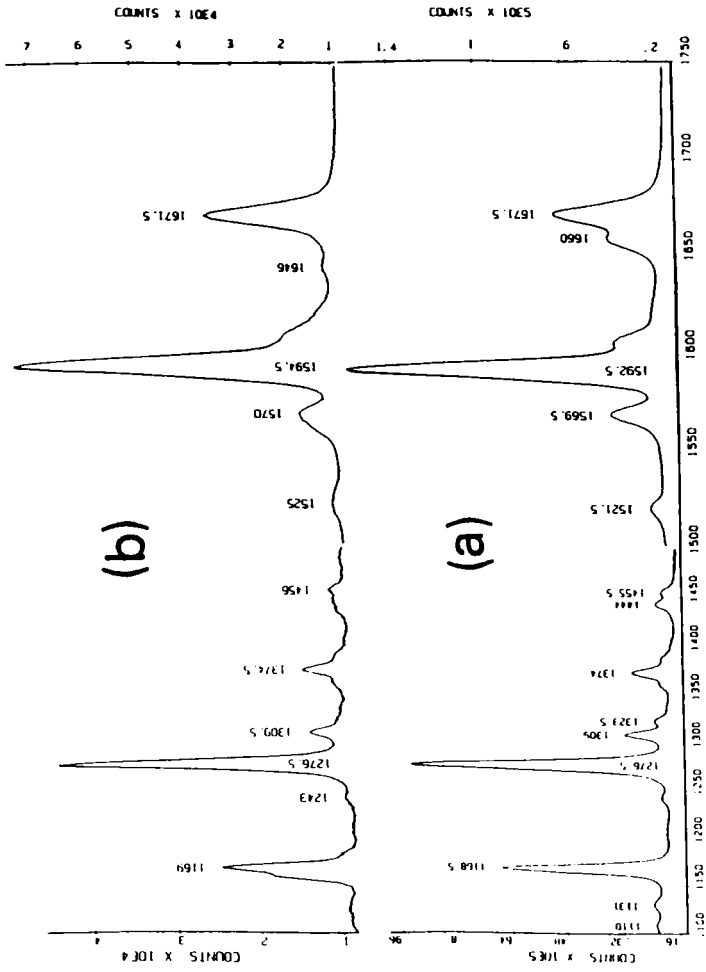

Fig 6 Raman spectra of PRC in the solid state between 1100 and 1750 cm^{-1} (a) non-deuterated, laser power = 300 mw and slits = 400 μm, (b) deuterated with laser power = 400 mw and slits = 400 μm.

Using the Krueger-Thompson relationship[15], the value $\nu_s(N\text{-}D)^{cal.} - \nu_s(N\text{-}D)^{exp.} = 47\ cm^{-1}$ is higher than in NH_2 group; hence the harmonic approximation is not followed in the *p*-amino group when the isotopic shift is produced. Accordingly, the values of the force constants $K_{NH} = 6.46 \times 10^5$ dyn cm^{-1}, $K_{ND} = 6.59 \times 10^5$ dyn cm^{-1} and $\hat{HNH}$ and $\hat{DND}$ angles $\theta_H = 115.5°$, $\theta_D = 118.9°$, based on the Linnett[17] equations, were obtained. The variation of the V_2 rotation barrier with deuteration (Table 2) suggests that, when isotopic changes are superimposed on a probable increase in the coupling between ν_s and ν_{as} vibrations, there is a real change in the geometry of amine group. This fact is in accordance with that observed in other local anaesthetics[5] and in several chlorinated derivatives of phenol[18], as well as agreeing with the results using the Krueger-Thompson relationship[15] in the ND_2 group: $\nu_s(N\text{-}D) = 723.4 + 0.682\ \nu_{as}(N\text{-}D)$. Thus, the value $\nu_s^{cal.} - \nu_s^{exp.} = 52\ cm^{-1}$ obtained is higher than that computed in NH_2 group.

The presence in the IR spectrum of other new bands at 3402 and 2518 cm^{-1} must be attributed to the ν(N-H) and ν(N-D) vibrations in partially deuterated NHD groups. Their frequency ratio $\nu(N\text{-}H)/\nu(N\text{-}D) = 1.351$ (1.350 in Raman) is in accordance[5] with the harmonic approximation. Similar relations in NH_2 and ND_2 groups for the antisymmetric and symmetric vibrations were also calculated, with values 1.335 and 1.378 respectively. The $\nu_{as}(N\text{-}H)_{NH2} - \nu(N\text{-}H)_{NHD}$ difference is larger than $\nu(N\text{-}H)_{NHD} - \nu_s(N\text{-}H)_{NH2}$ in agreement with a slightly higher contribution of the symmetric character in the N-H bond of the NHD group. The lower difference in $\nu_{as}(N\text{-}D)_{ND2} - \nu(N\text{-}D)_{NHD}$ than that obtained between $\nu(N\text{-}D)_{NHD} - \nu_s(N\text{-}D)_{ND2}$ is in agreement with a slight increment of the antisymmetric character in the N-D bond of the NHD group. A greater decrease in the intensity of the ν_s mode than in the ν_{as} with the isotopic shift is also observed.

Other internal vibrations of *p*-amino group: Apart from the stretching frequencies, the *p*-amino group has scissoring, rocking, wagging and torsional modes. Thus the frequencies at 1625 cm^{-1} (IR) and 1606 cm^{-1} (Raman) were

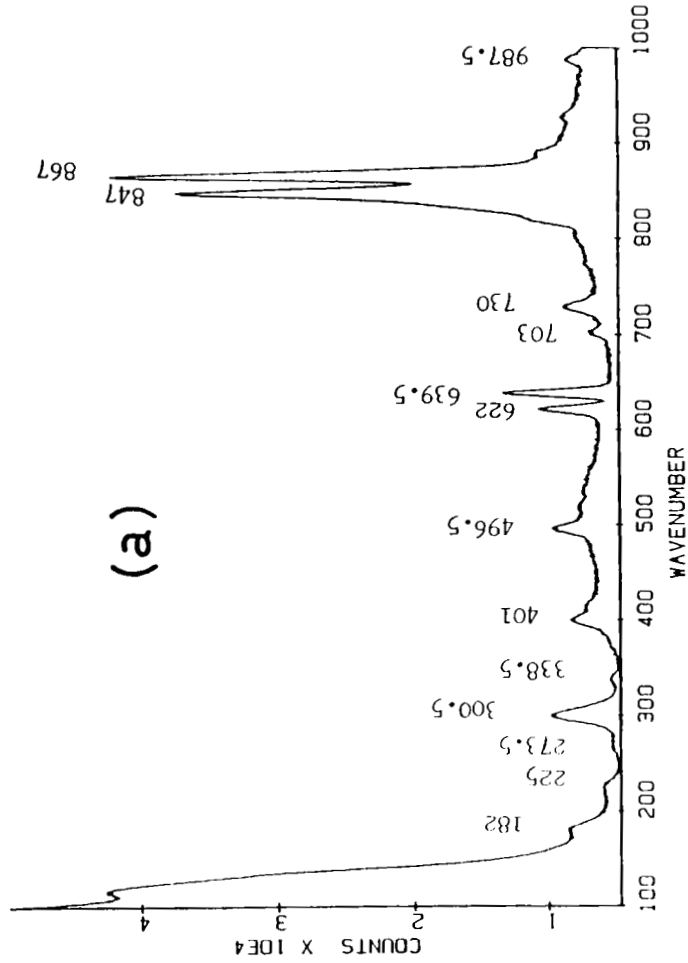

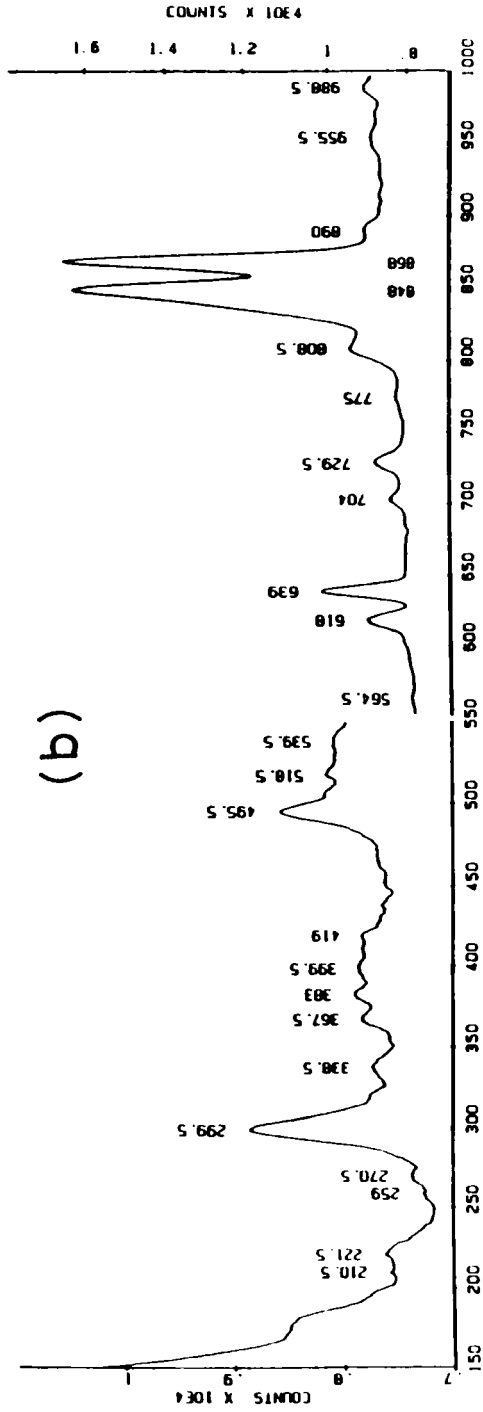

Fig. 7. Raman spectrum a) of the non-deuterated PRC in solid state between 100 and 1000 cm^{-1}, with laser power = 300 mw and slits = 400 μm. b) of the deuterated PRC in the solid state with laser power = 300 mw and slits = 400 μm.

Table 1. Frequencies observed, in cm^{-1}, intensity measured and assignment proposal for the bands of PRC.

Infrared				Raman		
solid		liquid		solid		Assignment
non-deut.	deuter.	75°C	175°C	non-deuter.	deuter.	
3458 vs	3450 s	3450 m	3460 m	3453.5 m	3455 vw	ν_{as}(N-H)
-	3402 s	-	-	-	3405 m	ν(N-H) in NHD
3360 vs	3358 s	3352 s	3360 s	3371.5 vs	3370 m	ν_{s}(N-H)
-	-	-	-	3300 m	-	$\nu(N\text{-}H\cdots)_{inter.}$?
3240 s	3240 w	3190 m	3205 vw	3234 m	-	$\nu(N\text{-}H\cdots)_{inter.}$?
3060 vw	-	-	-	3068 s	3069.5 s	ν(C-H) 20a
-	-	-	-	3054.5 m	3053.5 m	ν(C-H) 20a
3034 w	3034 w	-	-	3025.5 w	-	ν(C-H) 20b or 7b
-	-	-	-	2989.5 w	2990 w	ν_{as}(C-H) in CH_3
2962 s	2962 s	2950 s	2950 s	2950.5 vs	2950.5 vs	ν_{as}(C-H) in CH_2
2922 vw	2922 vw	2922 sh	-	2929 s	2929 s	ν_{as}(C-H) in CH_2
2862 m	2862 m	2862 sh	-	2871.5 m	2871.5 m	ν_{s}(C-H) in CH_2
2818 s	2818 m	2804 m	2804 m	2828 w	2828 w	ν_{s}(C-H) in CH_2
2675 w	2700 vw	2675 vw	-	-	-	ν(C=C) • $\Gamma(NH_2)$?
-	2590 s	-	-	-	2590 w	ν_{as}(N-D)
-	2518 s	-	-	-	2523 s	ν(N-D) in NHD
-	2438 s	-	-	-	2443 vs	ν_{s}(N-D)
2400 vw	-	-	-	-	-	$\beta_{s}(NH_2)$ + δ(CCC)?
2130 vw	-	2130 vw	-	-	-	$\tau(NH_2)$ + ν(C=C)?
1920 vw	1920 vw	1920 w	-	-	-	2γ(C-H)
1665 vs	1665 vs	1693 vs	1700 vs	1671.5 s	1671.5 s	ν(C=O)
-	-	-	-	1660 m	-	$\beta_{s}(NH_2)$?
1625 vs	1620 sh	1620 vs	1620 vs	1606 w	-	$\beta_{s}(NH_2)$
1600 vs	1600 vs	1598 vs	1598 vs	1592.5 vs	1594.5 vs	ν(C=C) 8a
1570 m	1570 w	1570 vw	1570 vw	1569.5 m	-	ν(C=C) 8b
1518 vs	1515 vs	1510 s	1510 s	1521.5 w	1525 vw	ν(C=C) 19a
1470 vw	1480 vw	-	-	-	-	ν(C=C) 19b
1453 s	1451 m	1448 sh	1452 w	1455.5 vw	1456 vw	δ_{as}(C-H) in CH_2
1442 s	1430 m	1432 m	1435 m	1444 w	-	δ_{as}(C-H) in CH_2
1380 s	1380 s	-	-	-	-	δ_{as}(C-H) in CH_2
1374 s	1372 s	1368 m	1375 m	1374 m	1374.5 m	δ_{s}(C-H) in CH_3
1368 s	1365 s	-	-	-	-	δ_{s}(C-H) in CH_3

Table 1. Continued

-	1355 sh	-	-	-	-	β_s(NDH) ?
-	1345 m	-	-	-	-	β_s(NDH) ?
1335 m	1332 m	-	-	-	-	δ(C-H) in ethyl group
1320 s	1318 m	-	-	1323.5 vw	-	δ(C-H) in ethyl group
1310 s	1308 s	1305 m	1305 m	1309 m	1309.5 w	ν(C-C)
1275 vs	1270 vs	1265 vs	1265 vs	1276.5 vs	1276.5 vs	ν(C-N), ν_{as}(C-O-C)
1242 sh	1240 sh	-	-	1243 vw	1243 vw	δ(C-H)
1205 m	1205 m	1198 w	1198 w	-	-	δ(C-H) in ethyl group
1170 vs	1168 vs	1167 vs	1167 vs	1168.5 vs	1169 s	δ(C-H)
-	1160 sh	-	-	-	1160 sh	$\beta_s(ND_2)$
1128 vs	1130 s	1108 s	1108 s	1131 vw	-	δ(C-H)
1110 w	1108 sh	-	-	1110 vw	-	δ(C-H)
1080 m	1078 w	1073 sh	-	-	-	$\Gamma(NH_2)$
1050 vw	1048 vw	-	-	-	-	δ(C-H)
1018 s	1018 s	1008 w	1008 vw	-	-	ν(C≡C), δ(C-C-C) ?
988 m	985 m	965 w	965 w	987.5 vw	988.5 vw	δ(C-H) in ethyl group
928 m	928 m	926 vw	-	927.5 vw	-	δ(C-H) ?
-	-	-	-	890 vw	890 vw	γ(C-H) in CH_3?
870 w	867 w	-	-	867 vs	868 vs	γ(C-H) 17b
842 s	842 s	840 s	840 s	847 vs	848 vs	γ(C-H), δ(COO)
805 w	805 vw	-	-	-	-	γ(C-H) in amine 3rd
773 vs	775 vs	770 s	768 s	775.5 vw	775 vw	γ(COO), δ(C-C-C) ?
728 m	728 m	730 w	730 w	730 w	729.5 w	δ(C-H) in ethyl group
703 s	703 s	695 m	695 m	703 w	704 w	γ(C-C-C) 4
640 m	640 m	639 w	639 w	639.5 s	639 s	δ(C-C-C) 6b
620 s	614 m	615 m	615 m	622 m	618 m	δ(C-N) in amine 3rd, δ(COO)
575 br	-	-	-	-	-	$\gamma(NH_2)$ wagging
-	-	-	-	-	564.5 vw	γ(NHD) wagging
535 w	535 w	-	-	536 vw	539.5 vw	δ(COO), δ(C-N) amine 3rd
-	516 sh	-	-	-	-	γ(NHD) wagging
508 s	508 s	506 m	506 m	519 vw	518.5 vw	γ(C-C-C) 16b
470 w	-	-	-	496.5 w	495.5 vw	$\gamma(NH_2)$ wagging
-	-	-	-	-	453 vw	$\gamma(ND_2)$ wagging
418 w	417 vw	-	-	414 vw	419 vw	δ(C-N)
-	400 br	-	-	-	-	$\gamma(ND_2)$ wagging
398 w	-	-	-	401 w	-	$\tau(NH_2)$ torsion
-	380 w			-	383 vw	γ(NDH) wagging

(continued)

Table 1. Continued

-	367 w	-	367.5 vw	$\gamma(ND_2)$ wagging
-	-	338.5 vw	338.5 vw	γ(C-C-C), γ(C-H)
-	340 vw	-	328 vw	τ(NDH) torsion
-	-	300.5 m	299.5 m	γ(C=O), γ(C-C-C)
-	-	273.5 vw	270.5 vw	γ(C=O), γ(C-N) ?
-	280 w	-	259 vw	$\tau(ND_2)$ torsion
		225 vw	221.5 vw	γ(C-C-C)
		182 w	182 vw	$\gamma(NH_2)$, γ(C-H)
		115 vw	115 vw	γ(C-H), γ(C-N)

Abbreviations: vs, very strong; s, strong; m, medium; w, weak; vw, very weak; sh, shoulder; inter, intermolecular; br, broad.

Table 2. Values of the experimental torsional frequencies (τ), rotational constants (B_o), and rotation barriers (V_2) in cm^{-1}, of the NH_2 group.

	Frequencies (τ)				$V_2^{opt.}$	
p-amino group	Exp.	CNDO/2	AM1	B_o	Harm. approx.	Hamilt. calc.
$-NH_2$	398 (IR)	243	322	10.2	3898	4124
	401 (R)				3957	4185
$-ND_2$	280 (IR)	176		5.0	3936	4010
	259 (R)				3368	3464

(IR) and (R), values obtained by infrared and Raman spectroscopy, respectively

interpretated as scissoring mode β_s in the NH_2 group. Their deuterated analogues were tentatively assigned to the band at 1160 cm^{-1}. With deuteration, due to NHD groups, bands were detected at 1355 and 1345 cm^{-1} corresponding to mode β_s(NHD). The mode rocking Γ was identified only in IR in the NH_2 group at 1080 cm^{-1}.

At 400 and 365 cm^{-1} in the IR spectrum of the deuterated compound very broad and weak bands appeared, having their correspondence in the non-deuterated spectrum at 575 and 470 cm^{-1}. Because of the form and the frequency of the bands which appeared, they were assigned to the wagging mode in the *p*-amino group. In the Raman spectrum they were identified in ND_2 at 495.5 and 367.5, and in NH_2 at 622 and 496.5 cm^{-1}. The relation in the frequencies $\gamma(NH_2)/\gamma(ND_2)$, ca. 1.36, was in accordance with the harmonic approximation. For the NHD group, wagging bands were also registered in the IR spectrum at 516 cm^{-1} (weak shoulder), and at 380 cm^{-1}. In Raman they were identified at 564.5 and 383 cm^{-1}.

The band corresponding to the torsional mode τ occured at 398 cm^{-1} in IR with weak intensity and its deuterated analogue at 280 cm^{-1}, $\tau(ND_2)$. The value of the NH_2/ND_2 ratio agrees with that reported in other local anesthetics[5]. The torsion vibration in NHD groups (Fig. 7) was identified in Raman at 328 cm^{-1}.

These assignments were within the frequency range given by Varsanyi[19,20] and are verified in other investigations[21-24].

C-N and COO vibrations: The C-N stretching vibration can be seen in various compounds[19,20] overlapped by other modes; thus the ν(C-N) in *p*-amino group and the ν_{as}(C-O-C) were observed in IR at 1275 cm^{-1}. The frequency of the carbonyl group ν(C=O) was registered in IR at 1665 cm^{-1}. In general, these bands were detected with very strong intensity in *p*-substituted benzoic acid derivatives[24,25].

The band at 418 cm^{-1} in IR was designated as δ(C-N), in the same way as the strong absorption at 620 cm^{-1}, to which a slight contribution of δ(COO) mode was also assigned.

C-H vibrations in saturated chain: The ν(C-H) stretching frequencies were observed in the 2800-3000 cm^{-1} range. In the Raman spectrum, the weak band at 2989.5 cm^{-1} corresponded to the antisymmetric mode in $-CH_3$, while those detected as strong and very strong intense bands at 2929 and 2950.5

cm^{-1} were ascribed to the $-CH_2-$ group. These bands appeared with higher intensity than IR. The vibrations at 2871.5 and 2828 cm^{-1} in the Raman spectrum were assigned to the symmetric mode in $-CH_2-$ groups.

Regarding the C-H in-plane bending vibrations, the IR absorptions at 1380, 1368, 1335, 1205 and 1050 cm^{-1} were not observed in the Raman spectra; while those at 1455.5, 1444, 1323.5, 1131, 987.5, 927.5 and 730 cm^{-1} decreased, appearing with weak or very weak intensity.

Overtones and combinations bands: In IR, the very weak bands which appeared at frequencies 1700-2700 cm^{-1}, that could not reasonably be assigned to fundamentals, may be combinations and overtones of normal modes, the assignments of which appear in Table 1. In the Raman spectra, as in the other local anesthetics studied[5], overtones and combination bands were not observed.

Normal vibrations of the ring:

A tentative assignment of the ring normal modes is shown in Table 1, according to Wilson's notation[20]. Vibrational analysis of benzoic acid derivatives have demonstrated the slight influence of the different substituents on the frequency of the ring normal vibrations. This fact allows the study of ring vibrations independently of the substituent internal modes.

In the tangential vibrations, the 8b and 19b carbon-carbon stretching modes appeared at higher frequencies and lower intensities than those which corresponded to 8a and 19a vibrations. Thus these last frequencies were identified as very intense IR absorptions at 1600 and 1518 cm^{-1} respectively (1592.5 and 1521.5 cm^{-1} in Raman), while 8b and 19b were assigned at 1570 cm^{-1} (1569.5 cm^{-1} in Raman) and 1470 cm^{-1}. These assignments were in the frequency intervals established elsewhere[19,20]. Other bands corresponding to δ(C-H) aromatic, within the frequency range 1250-1025 cm^{-1} were observed in the spectra.

The C-H stretching vibrations, corresponding to normal modes 20a, 20b and 7b, were in the 3000-3100 cm^{-1} range of the radial vibrations[19]; and to 20a

was assigned the very weak IR band at 3060 cm^{-1} (3068 and 3054.5 cm^{-1} in Raman), while the weak IR absorption at 3034 cm^{-1} (3025.5 cm^{-1} in Raman) was tentatively designated at 20b or 7b modes. These assignments find support in those reported on related molecules. Thus in methyl *p*-hydroxybenzoate[20], 7b and 20a were not identified due to their very weak intensity while 20b was observed at 3035 cm^{-1} as a weak absorption. None of these modes was distinguished in *p*-aminobenzoic acid[20]. The skeletal vibration δ(C-C-C) mode 6b was identified in IR at 640 cm^{-1} (639.5 cm^{-1} in Raman) while 6a was not detected in the spectra.

To the out-of-plane vibrations belong the skeletal vibrations 4, 16a and 16b of benzene. The frequency of the normal mode 4 is remarkably insensitive to substitution and appears very close to that of benzene, around 700 cm^{-1}. The strong intense band at 703 cm^{-1} was assigned to this mode. Vibrations 16a, 16b were within the 395-420 cm^{-1} and 455-570 cm^{-1} intervals respectively. The strong IR absorption at 508 cm^{-1} (519 cm^{-1} in Raman) was ascribed to the latter while the former was not observed in accordance with that described in related derivatives of benzene[20].

Among C-H out-of-plane vibrations, only normal mode 17b was able to be assigned in IR at 870 cm^{-1}, because the other vibrations have frequencies too low or intensities too weak to be observed clearly. In the Raman spectra mode 17b appeared with very strong intensity at 867 cm^{-1}.

LIQUID STATE

A study with the temperature between 25 and 175°C was carried out. Infrared spectra were recorded from 3500 to 400 cm^{-1}. Since the melting point of PRC is around 61°C, the spectrum recorded at 75°C (Fig. 3c) must correspond to the substance in the liquid phase which becomes embedded in the KBr matrix. Table 1 summarizes the results obtained in the solid phase at room temperature, and in the liquid phase in the proximity of the melting point, as well as at 175°C.

The main characteristics observed with the increment of the temperature in the vibrational pattern were the extension and the decrease of resolution in the bands due to thermal vibrations induced by heating. This fact makes difficult the detection of weak and very weak intensity bands and, they are therefore not included in the third and fourth columns of Table 1. The intermolecular interactions were clearly disminished when the temperature increased. Also noted was a weak displacement toward the low-frequency zone of all the bands, recovering a slight displacement in several when the sample crossed the melting point and with the increment of the temperature in this phase.

The following features were also distinguished between the IR spectra of the liquid and solid states:

A short displacement was observed in the frequencies of the stretching bands N-H, antisymmetric and symmetric, which appeared in liquid phase at 3450 and 3352 cm^{-1} respectively. When the sample passed to liquid state, the crystalline net was broken. However, the values of $K_{NH} = 6.46\ 10^5$ dyn cm^{-1} and $\hat{HNH} = 116.1°$, obtained using the Linnett equations[17], close to solid state values, indicated the slight influence of the crystalline net, and the considerable stability of the geometric parameters in the NH_2 group.

The intensity ratio between ν(N-H) bands was $I_{symm.}/I_{antisymm.} \simeq 1$ in the solid state in contrast to $I_{symm.}/I_{antisymm.} \simeq 1.3$ in the liquid state at 175°C, due to a decrease in the intensity of the antisymmetric higher than the symmetric vibration when the temperature increased. This fact was also noted in other local anesthetics[5].

A high decrease in the intensity of the torsional $\tau(NH_2)$ and wagging $\gamma(NH_2)$ modes was produced when the temperature increased; and they were extinguished when the sample was in the liquid phase, 75°C. Similar behavior was observed in the rocking mode $\Gamma(NH_2)$ at 1080 cm^{-1}, which disappeared with a slight increment of the temperature in the liquid state. These features were confirmed in other local anesthetics[5].

When the sample crossed the melting point, an increment ca. 28 cm^{-1} in the frequency of the band corresponding to the $\nu(C=O)$ mode and a decrease ca. 50 cm^{-1} in the frequency of the band at 3240 cm^{-1} were observed. This band at 3240 cm^{-1} also showed a continuing increase of the width and a remarkable loss of intensity in the liquid phase as the temperature increased.

Other bands also showed a remarkable sensitivity to the temperature, such as the vibrations in CH_2 groups at 2862, 1453 and 1380 cm^{-1} and in CH_3 and ethyl groups at 1368 and 1335, 1320, 928 cm^{-1} respectively. These bands decreased in intensity as the temperature rose, disappearing in several cases in the liquid phase. The ring stretching vibrations $\nu(C=C)$ at 1570 and 1018 cm^{-1} behaved similarly.

HINDERED ROTATION OF THE NH_2 GROUP

The rotational barrier V_2 corresponding to the torsional modes $\tau(NH_2)$ in the *p*-amino group was calculated for a hindered rotation potential function[25]:

$$V(\alpha) = V_2 / 2 \ (1 - \cos 2\alpha)$$

where α is the rotation angle. Thus, the hindered rotation Hamiltonian is solved by using the optimization procedure described elsewhere[26,27], and by computing the values of the rotation barrier, V_2 (seventh column in Table 2). This same procedure was also used employing a harmonic approximation (HA), sixth column. An increase in the values of V_2 was calculated with a Hamiltonian. The difference was increased with higher experimental torsional frequencies. Nevertheless, the differences with the HA were slight; therefore the HA can be considered acceptable for estimating V_2 because of its greater simplicity.

The torsional frequencies in the NH_2 group, calculated with the CNDO/2 and AM1 methods, are shown in the third and fourth columns of Table 2. In the case of CNDO/2, they were obtained by the potential function, solving the

torsional Schroëdinger equation[25]. These frequencies, which are valid for the gas phase, can therefore be used as a test for experimental assignments.

Although smaller, the CNDO/2 torsional frequencies followed the same trend as did the frequencies obtained experimentally for amino groups. The differences between τ^{exp} and $\tau^{CNDO/2}$ can be attributed to several causes, such as the unavoidable redshift implied by the transition from solid to gas, the inaccuracy of the CNDO/2 method itself, the electronic nature of the rotational barrier and, finally, the contributions of some interactions of the molecules within the crystalline net of the compound.

INVERSION BARRIER IN THE *P*-AMINO GROUP

The wagging bands observed in the spectra are combinations between torsion and wagging vibrations[28] which are active in IR. Since there is no selection rule for the transitions, all are possible. Thus a scheme with six of these models of the inversion transitions for the first four energy levels was established[29]. The selection of the most suitable model to the experimental data, inversion barrier and inversion angle, reveals the scheme of the inversion transitions and the IR and Raman frequencies in the low frequency region, < 200 cm^{-1}.

To obtain the inversion barrier and the inversion angle three methods were used:

(1) Using an Harmonic approximation (HA) with the experimental average frequency of wagging (ν_i), the barrier heights ($\hat{V}_i$) were calculated, Table 3. The equations used[28,29], calculate the values of the coefficients V_1^i and V_2^i. The inversion constant B_i was obtained through the crystallographic data and the value of the inversion angle ω_o experimentally reported[30] in aniline, 37.5°.

(2) With a torsional Hamiltonian (T.H.), $\hat{V}_i$ and ω_o were calculated together. The procedure[29] was as follows: The set of values of inversion

angles (between 10° and 40°) and V_1^i (between 60000 and 100000 cm^{-1}) obtained V_2^i values. Introducing this set of V_1^i and V_2^i values in a torsional Hamiltonian[25], the energy levels and wavefunctions were computed in each case. With these energy levels the different inversion transitions were determined. Curves were plotted[5b] for each transition and on these curves the two experimental vibrations of wagging were traced. These frequencies coincide at only one point, from which the optimum values of ω_o, V_1^i and V_2^i that appear in the third to fifth columns respectively of Table 4 were obtained, as well as other inversion transitions, columns six to nine. These values are listed in the first row and are associated with the follows scheme of transitions[29]:

$$\psi_o^s \rightarrow \psi_o^{as}, \quad \psi_o^s \rightarrow \psi_1^s, \quad \psi_o^{as} \rightarrow \psi_1^s \quad \text{and} \quad \psi_1^s \rightarrow \psi_1^{as}.$$

In the second row are shown the respective values corresponding to deuterated *p*-amino group. With the isotopic exchange a decrease, low in ω_o and even lower in the barrier height was noted. These values were also different from those computed by AM1 (34.17°, 1463 cm^{-1}) and CNDO/2 (51.8°, 3051 cm^{-1}) methods and agree with those reported in aniline[22,31]. The inversion potential function energy levels and optimum transitions established with the IR data are shown in Fig. 8a, while the wavefunctions for the first four energy levels are plotted in Fig. 8b.

(3) The third method employed was an Harmonic approximation of vibration (H.A.V.) which also calculated together $\hat{V}_1$ and ω_o. This procedure employed an approximation of a double symmetric hole which considers the inversion as a vibration movement of harmonic character of the nitrogen atom through the plane defined by the two hydrogens of *p*-amino group and masses centrum of the molecule excluding this group[29]. The final results are shown in Table 4, which correspond to the same scheme of transitions described in the torsional Hamiltonian.

In Table 4 the H.A.V. procedure shows an excessively low value for ω_o and high for $\hat{V}_1$, related to the amino group in aniline[30]. However, a better

Table 3. With an Harmonic Approximation (HA) in cm^{-1}

p-amino group	$\tilde{\nu}_i$	B_i	V_1^i	V_2^i	$\hat{V}_i$
$-NH_2$	509 (IR)	29.32	33924	-10690	456
	559 (R)		40916	-12893	550
$-ND_2$	383.5 (IR)	16.14	34984	-11024	471
	410 (R)		39985	-12600	538

IR and R, values obtained by infrared and Raman spectroscopy, respectively.

Table 4. Parameters found, in cm^{-1}, for the first four energy levels using a Torsional Hamiltonian (T.H.) and an Harmonic Approximation of vibration H.A.V.

Method used			ω_o(°)	V_1^i	V_2^i	$\hat{V}_i$	ν_1	ν_2	ν_4	ν_6
T.H.	$-NH_2$	IR	32.3	73189	-21611	508	105	575	470	445
		R	30.4	88000	-25507	482	125.5	622	496.5	493
	$-ND_2$	IR	30.2	70350	-20360	377	33	400	367	298
		R	27.2	99000	-27840	343	85.5	453	367.5	354
H.A.V.	$-NH_2$	IR	20.4	-	-	779	105	575	470	277
		R	18.8	-	-	870	125.5	622	496.5	320
	$-ND_2$	IR	24.0	-	-	777	33	400	367	155
		R	16.5	-	-	600	85.5	453	367.5	214

IR, infrared absorption. R, Laser-Raman spectroscopy.

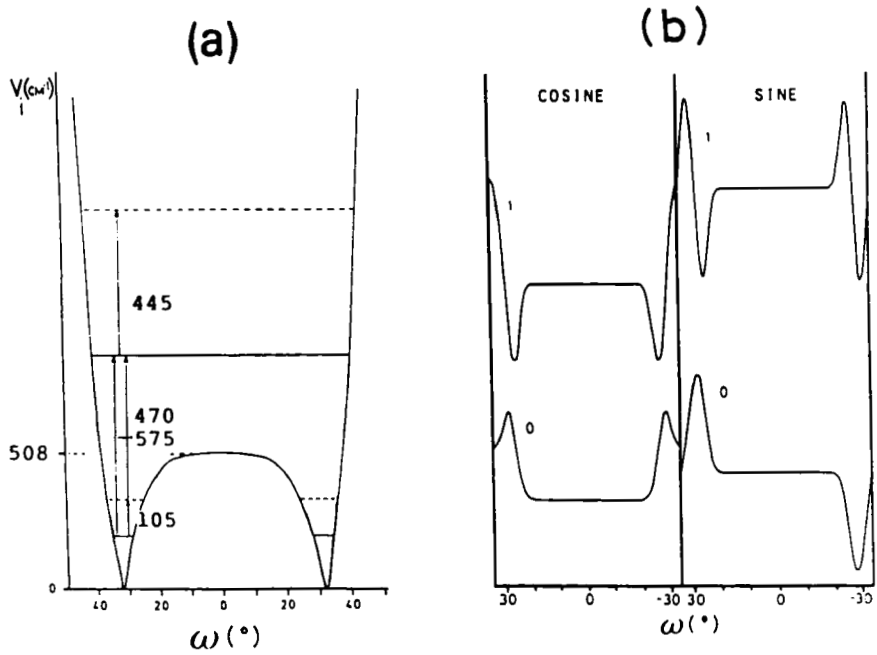

Fig. 8. a) Inversion potential function, energy levels and optimum transitions with a torsional Hamiltonian. b) Wavefunctions for the first four energy levels.

agreement was obtained with the H.T. method. This result was a consequence of the slight difference of energy that H.A.V established between the levels $\psi_o^s \rightarrow \psi_o^{as}$ and $\psi_1^s \rightarrow \psi_1^{as}$.

SUMMARY AND CONCLUSIONS

The bands of the IR and Raman spectra of PRC were assigned. Special attention was centered on the *p*-amino vibrations. Thus, with relations

ν(NH)/ν(ND) previously reported in related molecules, the bands corresponding to this group were identified and assigned. The frequencies of the vibration bands due to the two conformations of NHD group were also determined and that they obeyed the isotopic change rules was verified. The identification of partially deuterated NHD groups was in accordance with that observed in aniline derivatives.

The NH_2 and ND_2 torsional modes, inactive in IR according to the conventional selection rules, but observed in the spectra, were interpreted as symmetric and antisymmetric combination bands of the pure torsional mode with the first inversion transition. The inversion transitions between the first four energy levels, and the wagging bands in the far IR were determined.

In the study concerning the temperature of the IR spectrum, when the sample reached the melting point, a sudden change in the intensity of the bands was noted, especially in the NH stretching modes.

Several procedures were used to obtain the barrier height and the inversion angle. These results complete the theoretical study and are in good accordance with those published earlier.

ACKNOWLEDGEMENTS

The author acknowledges and appreciates the co-operation of Instituto de Optica *Daza de Valdes* del CSIC of Madrid, for the facilities for IR and Raman spectra. Thanks are also due to Dr. J.L. Nuñez and Dras. J. Abellanato, C.S. Sigüenza and M. Santos for their interest, help and encouragement.

REFERENCES

1. F.E. Brown and M.J. Halsey, *Molecular Mechanisms of Anaesthesia, Progress in Anesthesiology*, vol. 2, Raven Press., New York (1980).
2. A.M. Casanovas, C. Labat, P. Courriere and J. Austin, *Eur. J. Med. Chem. -Chim. Ther.*, **17**, 4, 333 (1982).
3. (a) M. Remko and J. Cizmarik, *Acta Fac. Pharm. Univ. Comenianae*, **40**, 21 (1986). (b) J. Gerhards, T.-K. Ha and X. Perlia, *Arzneim.-Forsch*, **36**, 5, 861 (1986).

4. (a) M. Remko, J. Veselovska and J. Cizmarik, *Cesk. Farm.*, **36**, 5, 212 (1987). (b) G. Vergoten, G. Fleury and A.P. Gamot, *J. Raman Spectry.*, **14**, 6, 371 (1983). (c) E.C. Kelusky and I.C.P. Smith, *Biochemistry*, **22**, 25, 6011 (1983).

5. (a) M. Alcolea Palafox, *J. Raman Spectry.*, **20**, 765 (1989); *Spectrochim. Acta*, **44 A**, 12, 1465 (1988). (b) *Indian J. Pure & Appl. Phys.*, **30**, 59 (1992) and **31**, 90 (1993); *Spectrosc. Letters*, **26**, 8, 1395 (1993).

6 (a) S. Kashina, M. Ikeda and M. Haisa, *Acta Cryst.*, **38 B**, 1868 (1982). (b) B.K. Sinha, E. Subramanian, V. Pattabhi and J. Trotter, *Indian J. Pure & Appl. Phys.*, **22**, 4, 249 (1984).

7. (a) P.C. Dideberg, J. Lamotte and L. Dupont, *Acta Cryst.*, **36 B**, 1500 (1980). (b) G.R. Freeman and Ch. E. Bugg, *Acta Cryst.*, **31 B**, 96 (1975). (c) D.D. Dexter, *Acta Cryst.*, **28 B**, 77 (1972).

8. (a) H.G. Mautner, *Molecular and Quantum Pharmacology*, Eds. E. Bergmann and B. Pullman, D. Reidel, Dordrecht (1974). (b) M. Remko and P. Th. Van Duijnen, *J. Mol. Struct. (Theochem.)*, **14**, 1-2, 1 (1983).

9. R.A. Kydd and P.J. Krueger, *Chem. Phys. Lett.*, **49**, 539 (1977).

10. M.J.S. Dewar, E.G. Zoebisch, E.F. Healy and J.J.P. Stewart, *J. Am. Chem. Soc.*, 107, 3902 (1985).

11. M.J.S. Dewar and J.J.P. Stewart, *Q.C.P.E. Bull.*, 6, 506 (1986).

12. D.A. Liotard, E.F. Healy, J.M. Ruiz and M.J.S. Dewar, ***AMPAC MANUAL. Version 2.1. A general molecular orbital package***, Ed. R.D. Dennington II and E.F. Healy, Univ. of Texas at Austin (1989).

13. J.A. Pople and D.L. Beveridge, *Approximate Molecular Orbital Theory*, McGraw-Hill, New York, 1970.

14. D.M. Strorch, *Draw: molecule drawing program*, Dewar group, Univ. of Texas at Austin (1984).

15. P.J. Krueger and H.W. Thompson, *Proc. R. Soc. London*, Ser. **250 A**, 22 (1959).

16. G. Brink and J.W. Bayles, *Spectrochim. Acta.*, **30 A**, 835 (1974).

17. L.J. Bellamy, *Advances in Infrared group frequencies*, Methuen, London (1968).

18. Y.G. Smeyers and A. Hernandez-Laguna, *J. Mol. Struct.*, **149**, 127 (1987).

19. G. Varsanyi, *Vibrational spectra of bencene derivatives*, Academic Press, New York (1969).

20. G. Varsanyi, *Assignment for vibrational spectra of seven hundred benzene derivatives*, Adam Hilger, London (1974).

21. J.C. Evans, *Spectrochim. Acta*, **16**, 428 (1960).

22. Z. Niu, K.M. Dunn and J.E. Boggs, *Mol. Phys.*, **55**, 2, 421 (1985).

23. G.N.R. Tripathi, *J. Chem., Phys.*, **73**, 11, 5521 (1980).

24. S.K. Singh and R.N. Singh, *Indian J. Pure Appl. Phys.*, **21**, 744 (1983).
25. J.D. Lewis, T.D. Malloy, J.R. Tainer, T.H. Chao and J. Laane, *J. Mol. Struct.*, **12**, 427 (1972).
26. A. Brauler, E. Mathier, R. Meyr, M. Ribeaud and H.H. Gunthard, *Mol. Phys.*, **15**, 597 (1968).
27. M. Onda, T. Motoda and I. Yamaguchi, *Bull. Chem. Soc. Jpn.*, **58**, 242 (1985).
28. N.W. Larsen, E.L. Hansen and F.M. Nicaleisen, *Chem. Phys. Letters*, **43**, 584 (1976).
29. M. Alcolea Palafox, *J. Mol. Struct.*, **175**, 81 (1988).
30. D.G. Lister, J.K. Tyler, J.H. Hog and N.W. Larsen, *J. Mol., Struct.*, **23**, 253 (1974).
31. Z. Niu and J.E. Boggs, *J. Mol. Struct. (Theochem.)*, **109**, 381 (1984).

Date Received: February 10, 1994
Date Accepted: March 11, 1994